

Equilibrium Beam Distribution and Halo in the LHC

R. Assmann, F. Schmidt, F. Zimmermann, CERN, Geneva, Switzerland; M.-P. Zorzano, INTA, SPAIN

Abstract

The equilibrium LHC beam distribution at large amplitudes is a crucial input to the collimation and machine protection design, as well as to background studies. Its estimation requires a knowledge of the diffusion rates at which beam particles are transported to large transverse or longitudinal amplitudes. Important known mechanisms of particle diffusion include Touschek scattering, synchrotron radiation, intrabeam scattering (IBS), the nonlinear motion due to the long-range (LR) beam-beam (BB) collisions at top energy, persistent-current field errors during injection and at the start of acceleration, and Coulomb scattering off the residual gas. We summarize the expected contributions from different sources, introduce a diffusion model, and illustrate the evolution of the beam distribution at 7 TeV.

1 INTRABEAM SCATTERING

The transverse particle position at location s is related to the action variable I via $x = \sqrt{2\beta(s)I} \cos \phi(s)$, where $\phi(s)$ denotes the betatron phase, and $\beta(s)$ the beta function. The average action equals the rms beam emittance $\langle I \rangle = \epsilon$. We estimate the action drift due to IBS as

$$\left\langle \frac{\Delta I}{\Delta t} \right\rangle \approx \frac{\epsilon_{x,0}}{\tau_{\text{IBS},x}} \approx 1.5 \times 10^{-15} \text{ms}^{-1}, \quad (1)$$

using $\tau_{\text{IBS},x} \approx 94$ hr (at 7 TeV with 16 MV rf voltage) and $\gamma\epsilon_{x,0} \approx 3.75 \mu\text{m}$, and the associated diffusion coefficient as

$$D_{\text{IBS}}(I) \approx 2I \langle \Delta I / \Delta t \rangle \approx 2.9 \times 10^{-15} I \text{ms}^{-1}. \quad (2)$$

At injection, $\tau_{\text{IBS},x} \approx 44$ hr, and $D_{\text{IBS}}(I) \approx 6.3 \times 10^{-15} I \text{ms}^{-1}$.

2 GAS SCATTERING

The diffusion due to Coulomb scattering off the residual gas is described by

$$D_{\text{gs}}(I) = I\beta \left\langle \frac{\Delta\theta^2}{\Delta t} \right\rangle = I\beta \left(\frac{14.1 \text{MeV}/c}{p} \right)^2 \frac{\rho c}{X_0}, \quad (3)$$

where β is the average beta function (about 100 m), X_0 the radiation length of the gas and ρ its density.

The LHC ‘design gas density’ is derived for a 100 hr lifetime due to nuclear interactions [1]. Consider as an example an H_2 density of 10^{15} molecules per m^3 [1]. With $X_0 \approx 610 \text{kg m}^{-2}$, at 7 TeV one finds $D_{\text{gs}}(I) \approx 6 \times 10^{-16} I \text{ms}^{-1}$, smaller than the diffusion expected from IBS by a factor of 5. The corresponding emittance lifetime

is 500 hrs. If we consider instead CO ($X_0 \approx 362 \text{kg m}^{-2}$) at a density of $1.3 \times 10^{14} \text{m}^{-3}$, also compatible with the 100 hr beam lifetime, we get $D_{\text{gs}}(I) \approx 2 \times 10^{-15} I \text{ms}^{-1}$ or an emittance lifetime of 150 hr. At injection energy this would decrease to 40 minutes. Fortunately, this CO pressure is considered as unlikely to occur in the LHC [1].

3 LONG-RANGE BEAM BEAM

The dominant diffusion mechanism at large amplitudes is the effect of the long-range collisions. At 7 TeV the two beams are separated by about 9.5σ during $n_{\text{par}} = 30$ long-range encounters around each of the two main interaction points (IPs).

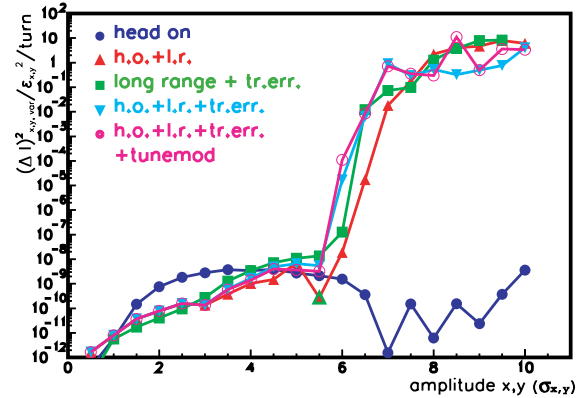


Figure 1: Change of action variance per turn vs. start amplitude $x_{\text{start}} (= y_{\text{start}})$ in units of rms beam size for two IPs [2].

As an example, Fig. 1 illustrates the diffusion rate computed by a weak-strong beam-beam simulations as a function of amplitude. Note that a ‘1’ on the vertical axis refers to $\Delta I^2 / \Delta t \approx 3 \times 10^{-15} \text{m}^2/\text{s}$ or to $\Delta x \approx 2.3 \text{mm}$ in $\Delta t \approx 1 \text{s}$ at $\beta = 100 \text{m}$.

There is a clear threshold (‘diffusive aperture’) at an amplitude of about $6\sigma_{x,y}$. Beyond this aperture, the motion is strongly chaotic and the diffusion here can be described by the analytical expression [3]

$$D_{\text{lr}}(I) = \frac{K^2 f_{\text{rev}}}{2} \frac{1}{A-1} f(A), \quad \text{where} \quad (4)$$

$f(A) = \left[A^3 - A^2 + 4A^2 \sqrt{\frac{1-A}{1+A}} - 6A + 6 - 6\sqrt{\frac{1-A}{1+A}} \right]$, $A = \sqrt{2I/\beta^*}/\theta_c$, and $K = 2r_p N_b n_{\text{par}}/\gamma$. For the LHC $\beta^* = 0.5 \text{m}$, $f_{\text{rev}} = 11 \text{kHz}$ (revolution frequency), $\theta_c = 300 \mu\text{rad}$ (crossing angle), $N_b = 1.1 \times 10^{11}$, $n_{\text{par}} = 30$ (considering 1 IP), $r_p \approx 1.5 \times 10^{-18} \text{m}$, $\gamma \approx 7461$. At small amplitudes the motion is regular, and in this case the

estimated diffusion coefficient (4) can be regarded as an upper bound.

4 DIFFUSION MODEL

We approximate the evolution of the beam distribution $f(I)$ by a diffusion equation

$$\frac{\partial f}{\partial t} = \frac{\partial}{\partial I} \left(D(I) \frac{\partial f}{\partial I} \right). \quad (5)$$

Further we assume that below 6σ ($I/\epsilon < 18$) the diffusion coefficient is dominated by intrabeam scattering, approximated by Eq. (2), and that, if the second beam is present, above 6σ it is due to long-range collision, and described by Eq. (4). The change in $D(I) = D_{IBS}(I) + D_{lr}(I)$ is discontinuous. The diffusion coefficient so obtained is illustrated in Fig. 2.

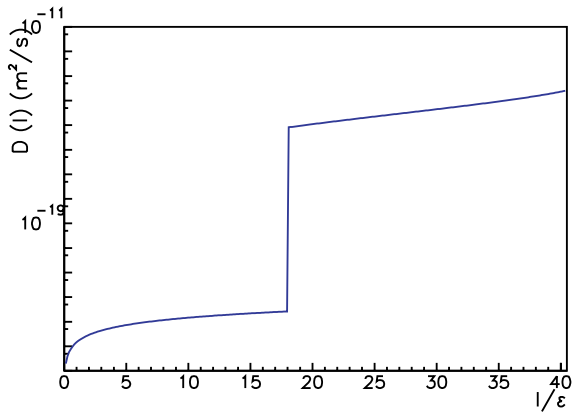


Figure 2: Model diffusion coefficient vs. normalized action, representing the combined effect of intrabeam scattering and long-range collisions.

The primary collimators may be represented by an absorbing boundary, if we neglect the re-scattering probability of about 1%.

5 TIME EVOLUTION

We assume that the closest collimator is located at 7σ . For $I = 0$ we choose a reflecting boundary. The initial beam distribution is taken to be exponential in the action variable of the form $\exp(-I/\epsilon)$ (here ϵ is the rms emittance). We integrate Eq. (5) in time, following a procedure similar to that described in [4].

Figure 3 shows the total number of protons lost on the collimators as a function of time. Most of the diffusion is due to intrabeam scattering. It takes about 60 hours before particles are transferred near the diffusive aperture. After 90 hours the long-range collisions increase the total losses by about 30%.

The effect of the long-range collisions becomes much more pronounced, if we increase the core diffusion rate. A factor of about two increase in the diffusion rate may be expected from gas scattering, if the CO molecular density

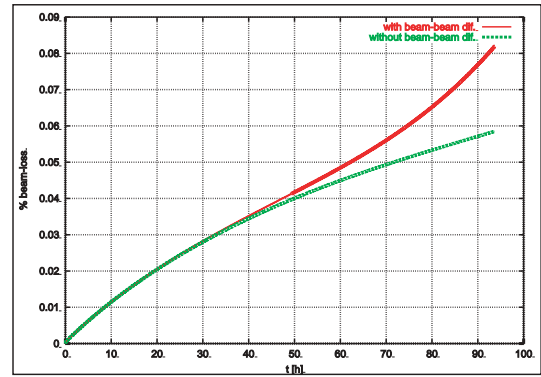


Figure 3: Fraction of protons lost vs. time in hrs with intra-beam scattering only (lower curve) and if diffusion due to long-range beam-beam forces is also included (top curve).

is $1.3 \times 10^{14} \text{ m}^{-3}$. As a more pessimistic scenario, we consider a factor 30 increase in the core diffusion rate. In this case, with or without long-range collisions, after roughly 6 hours the emittance is 3 times larger than at the beginning. From that moment on a much higher particle density is incident on the collimator. With long-range collisions present, after 16 hr 10% of the beam has been lost on the collimators, which is about two times more than without the long-range collisions. However, radiation damping at 7 TeV, not included in the model, will reduce the losses.

Figure 4 displays the beam distribution at various times during the store for the nominal configuration and for the 30 times larger core diffusion rate, respectively. The left pictures represent the effect of intrabeam or gas scattering alone, the right picture includes the long-range collisions. The latter clearly deplete the beam halo at large amplitudes. These distributions provide information on the beam loss at the collimators in case of orbit motion.

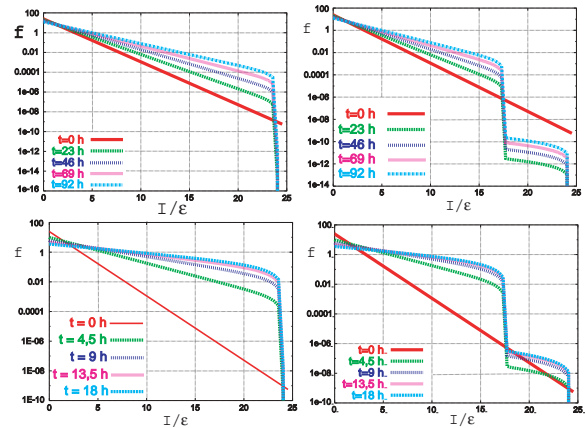


Figure 4: Density distributions at various times without (left) and with (right) diffusion due to long-range beam-beam forces, for the nominal case (top) and for enhanced core diffusion (bottom).

6 CHAOTIC DIFFUSION AT 450 GEV

Also at injection, the long-range collisions induce diffusion. Since here the beams are separated further (by $12-14\sigma$) the diffusive aperture is found at a larger amplitude (in units of σ) than at 7 TeV. The nonlinear fields of the superconducting magnets introduce additional nonlinearities. We have simulated the diffusion due to the combined effect of field errors and LR-BB using the SixTrack code. For 60 error random seeds, we have tracked groups of 60 particles launched at different starting amplitudes, with slightly different initial conditions, and computed the evolution of action spread and the maximum amplitude growth in each group. Results for the worst random seed are displayed in Fig. 5. We show the rise in amplitude in the left part of the figure. Besides a very steep amplitude increase at amplitudes larger than 10σ there is also a considerable amplitude increase and particle loss at 7σ . It is interesting to note that these losses come from particles in small chaotic nests located within otherwise stable regions and that this effect is much enhanced when the long-range collisions are taken into account. Correspondingly (right part of the figure), the diffusion rates are large in the regions with amplitude rise and there is no diffusion in the stable regime.

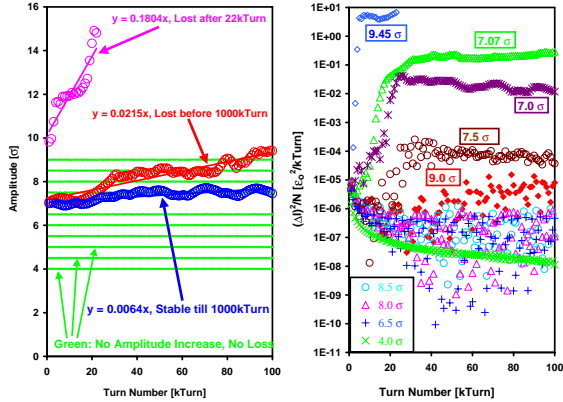


Figure 5: Simulated amplitude increase and diffusion vs. starting amplitude, at 450 GeV, illustrating the effect of long-range beam-beam forces and field errors.

7 TOUSCHEK SCATTERING

Touschek scattering is a longitudinal loss mechanism which can create a significant component of uncaptured ‘coasting’ beam. The Touschek scattering rate is described by [5] $dN_b/dt = -\alpha N_b^2$, giving rise to a coasting beam component of $N_{coast} = \alpha N_0 t / (1 + \alpha N_0 t) N_0$. For round beams, the coefficient α equals [6]

$$\alpha_{rd} = \frac{\pi r_p^2 c}{\gamma^4} \frac{\beta_x \beta_y}{\sigma_x \sigma_y V \eta} g\left(\frac{\delta q}{\eta}\right) \quad \text{with}$$

$$g(\epsilon) = \sqrt{\epsilon} \int_{\epsilon}^{\infty} \frac{e^{-u}}{u^{3/2}} \left(\frac{u}{\epsilon} - 1 - \frac{1}{2} \ln \frac{u}{\epsilon} \right) du$$

where $r_p (= 1.5 \times 10^{-18} \text{ m})$, $V = 8\pi^{3/2} \sigma_x \sigma_y \sigma_z$, $\eta = (\Delta E/E)_{\max}$, $\delta q = \gamma \sigma_x / \beta_x$.

The nominal LHC design [7] foresees two rf systems with total voltages and harmonic numbers equal to $\hat{V}_{rf,1}$ ($h = 35640$) = 750 kV (16000 kV), $\hat{V}_{rf,2}$ ($h = 17820$) = 3000 kV (0 kV) where the first numbers refer to injection and the values in parentheses to top energy.

This yields [8] $\alpha_{rd} \approx 5.0 \times 10^{-19} \text{ s}^{-1}$ at injection, and $\alpha_{rd} \approx 2.0 \times 10^{-19} \text{ s}^{-1}$ at 7 TeV. These numbers have been confirmed [8] using the more general formula by Piwinski [9], which applies to beams of arbitrary aspect ratio.

A coasting beam component is produced at rate per proton of $1.8 \times 10^{-4} \text{ hr}^{-1}$ (inj.) and $8 \times 10^{-5} \text{ hr}^{-1}$ (at 7 TeV). Particles outside of the rf bucket lose energy due to synchrotron radiation at a rate $d\delta/dt \approx -2.8 \times 10^{-9} \text{ s}^{-1}$ at injection, and $d\delta/dt \approx -1.0 \times 10^{-5} \text{ s}^{-1}$ at top energy. Since the energy aperture provided by the collimators is 3.9×10^{-3} [10], a scattered proton is lost after $\tau_{loss} \approx 390$ hrs (injection) or $\tau_{loss} \approx 6.5$ minutes (at 7 TeV), and at 7 TeV we expect a steady-state coasting beam fraction of $\alpha_{rd} N_0 \tau_{loss} \approx 10^{-5}$.

8 CONCLUSIONS

After storing the beam for 1 hour at injection a fraction of 2×10^{-4} of the beam is outside of the rf bucket due to Touschek scattering. In collision, the Touschek effect leads to a proton loss rate of 10^{-4} hr^{-1} , and to a steady coasting-beam component of about 10^{-5} .

Beyond the transverse diffusive aperture of about 6σ , induced by the LR-BB interaction, particles are lost rapidly. A transverse diffusion model predicts the loss rate and the time evolution of the transverse beam distribution caused by the combined action of IBS, gas scattering and LR beam-beam. The results of a numerical solution indicate how the LR collisions affect the shape of the beam halo.

Finally, an investigation of the diffusion at injection included the effects of LR encounters and magnet field errors. In this case, there is no clear border between regular and unstable regions of phase space, and particles in chaotic ‘nests’ can be lost rapidly. Modelling this situation will require an extension of the diffusion model to higher dimensions.

9 REFERENCES

- [1] N. Hilleret, private communication (2002).
- [2] Y. Papaphilippou *et al.*, PRST-AB 2, 104001 (1999).
- [3] Y. Papaphilippou, F. Zimmermann, ‘‘Estimates of Diffusion due to Long-Range Beam-Beam Collisions,’’ in preparation.
- [4] M.-P. Zorzano and T. Sen, LHC-PROJECT-NOTE-222 (2000).
- [5] C. Bernadini *et al.*, PRL, vol. 10, p. 407 (1963).
- [6] Y. Miyahara, Jap. J. Appl. Phys., vol. 24, p. L742 (1985).
- [7] E. Shaposhnikova, private communication (2000).
- [8] F. Zimmermann, M.-P. Zorzano, LHC Project Note 244 (2000).
- [9] A. Piwinski, DESY 98-179 (1998).
- [10] D. Kaltchev, private communication (2000).